Mechanical Limits of Bacterial Flagellar Motors Probed by Electrorotation

Richard M. Berry, Linda Turner, and Howard C. Berg
Rowland Institute for Science, Cambridge, Massachusetts 02142 USA

ABSTRACT We used the technique of electrorotation to apply steadily increasing external torque to tethered cells of the bacterium *Escherichia coli* while continuously recording the speed of cell rotation. We found that the bacterial flagellar motor generates constant torque when rotating forward at low speeds and constant but considerably higher torque when rotating backward. At intermediate torques, the motor stalls. The torque-speed relationship is the same in both directional modes of switching motors. Motors forced backward usually break, either suddenly and irreversibly or progressively. Motors broken progressively rotate predominantly at integral multiples of a unitary speed during the course of both breaking and subsequent recovery, as expected if progressive breaking affects individual torque-generating units. Torque is reduced by the same factor at all speeds in partially broken motors, implying that the torque-speed relationship is a property of the individual torque-generating units.

INTRODUCTION

Many species of bacteria swim by means of rotating helical filaments. These filaments are driven at their base by a reversible rotary motor embedded in the cell envelope. Bundles of filaments in swimming cells of *Escherichia coli* rotate at speeds on the order of 100 Hz (Lowe et al., 1987), whereas cells tethered to a surface by a single filament (Silverman and Simon, 1974) can rotate in either direction at approximately equal speeds, on the order of 10 Hz (Berg, 1974). The flagellar motor of this species is powered by the flux of H^+ ions down an electrochemical gradient into the cell across the cytoplasmic membrane. The filament connects via the hook and rod to the MS- and C-rings, where torque generation is thought to occur. Each motor has several independent torque-generating units containing the proteins MotA and MotB (Block and Berg, 1984; Blair and Berg, 1988), which correspond to studs seen in rings in freeze-fracture electron micrographs of the cell envelope (Coulton and Murray, 1978; Khan et al., 1988). For recent reviews of the bacterial flagellar motor, see Blair (1990), Jones and Aizawa (1991), Macnab (1992), and Schuster and Khan (1994).

The mechanical properties of the motor are best understood in terms of the relationships between ion flux and ion motive force (whose product gives the input power) and torque and speed (whose product gives the output power). In *Streptococcus* and *E. coli*, torque is proportional to proton motive force (Manson et al., 1980; Conley and Berg, 1984; Khan et al., 1985; Khan et al, 1990; Fung and Berg, 1995), and the proton flux coupled to rotation corresponds to ~ 1200 protons per revolution (Meister et al., 1987). Recently, using an electrorotation method first applied to bacteria by Washizu et al. (1993), Berg and Turner (1993) measured the relationship between torque and speed in tethered cells of *E. coli* at speeds up to several hundred Hz in either direction. They studied cells of a strain deleted for the response regulator, CheY, which spin exclusively counterclockwise (CCW), and found that torque in the CCW or forward direction was approximately constant up to speeds ranging from 60 to 200 Hz, depending on temperature. At higher speeds, the torque declined. They also found a barrier to backward rotation: torques ranging from 1.2 to 4.3 times the stall torque were required to drive the motor backward. Motors that were driven backward past this barrier usually broke. Catastrophic breaks reduced the motor torque suddenly and irreversibly to zero, whereas progressive breaks reduced the motor torque incrementally and allowed cells to recover.

Our primary aim in this work was to investigate more closely the behavior of flagellar motors when they were driven backward. We made continuous recordings of the speed of tethered cells while using electrorotation to apply steadily increasing torques. This allowed us to observe cells before, during, and after breaking. Using a chemotactic mutant whose motors spin only CCW, we found that motors forced to spin backward generate high and approximately constant torque before they break. Switching cells of a strain wild-type for chemotaxis showed the same torque-speed relationship in both directional modes. The torque-speed relationship obtained from partially (progressively) broken motors had the same shape as that obtained from the same motors before they are broken, with torque reduced by a constant factor at all speeds tested. This indicates that the torque-speed relationship is a property of individual torque-generating units. Motors that were broken progressively recovered in steps similar to those seen in genetic resurrection experiments with the proteins MotA and MotB, confirming the hypothesis that progressive breaking involves destruction or removal of independent torque-generating units. In progressively broken switching cells, both directional modes recovered simultaneously.

Received for publication 27 February 1995 and in final form 20 April 1995.

Address reprint requests to Dr. Howard C. Berg, Rowland Institute for Science, 100 Edwin Land Blvd., Cambridge, MA 02142. Tel.: 617-497-4656; Fax: 617-497-4627; E-mail: berg@risvax.rowland.org.

0006-3495/95/07/280/07 $2.00

MATERIALS AND METHODS

All methods were as described previously (Berg and Turner, 1993), except as noted below. Cells were tethered to glass rather than to SiO-coated sapphire. Experiments were run at room temperature. Data were acquired using LabVIEW version 3.0 (National Instruments, Austin, TX). The value of the applied torque was recorded in parallel with the data on cell angle acquired from the linear-graded filter apparatus. The acquisition rate was 1 kHz. These data, comprising photomultiplier output voltages X and Y, correspond to the x- and y-positions of the center of mass of the cell image. In most cases (for all figures except Fig. 5), groups of two or four consecutive points in X and Y were averaged, and signals were normalized to $+1$ at the peaks and -1 at the troughs, giving the cosine and sine of the cell angle, θ. θ was calculated as arc $\tan(\sin\theta/\cos\theta)$ and smoothed further by averaging 10 or 20 consecutive points. Finally, the rotation speed (in Hz) was calculated as $(1/2\pi)\, d\theta/dt$, using a second-order difference equation (Fröberg, 1969). For Fig. 5, rotation speeds were determined by the positions of peaks in the power spectra of successive blocks of data, each 8 s long, of the complex signal $Z = X + iY$. This method gave the sign as well as the magnitude of the speed, whereas power spectra of the signals X and Y give only the magnitude.

RESULTS

Symmetric clockwise (CW) and CCW torque-generating modes

It has been known for a long time that tethered cells of *E. coli* can rotate at approximately equal speeds in either direction (Berg, 1974). This implies that under conditions of high viscous load, CW and CCW modes generate approximately equal torque. Therefore, one might ask whether the dependence of torque on speed is the same in either mode at higher speeds. By applying external torque in both directions to tethered cells of *E. coli* strain KF84 (wild-type for chemotaxis) while the cells switched between CCW and CW modes, we found that this is indeed the case, at least for speeds up to ± 50 Hz.

The torque-speed relationship was pieced together from runs of the sort illustrated in Fig. 1. Initially this cell spun under its own power at about -7 Hz (CW), switching to $+7$ Hz (CCW) at $t = 1$ s and back into the CW mode at $t = 2$ s. Starting at $t = 2$ s, an increasing CCW torque was applied (Fig. 1 *a*), which slowed the cell and brought it to a halt at $t = 4$ s (Fig. 1 *b–d*). The cell remained stalled in the CW mode until $t = 5.5$ s, when it switched into the CCW mode. At this point the external torque and the motor torque were acting in the same direction, and the cell spun between $+20$ and $+30$ Hz. When the external torque was removed at $t = 7$ s, the cell spun at ± 7 Hz, as in the beginning.

Several records were made for each cell, with applied torques varying over different ranges, and the data were plotted together, with speed as a function of applied torque, as shown in Fig. 2. The two rotational modes appear as distinct curves in Fig. 2, *a* and *b*, the upper curve corresponding to intervals during which the cell exerted CCW torque, the lower curve to intervals during which the cell exerted CW torque. Clearly, both modes show resistance to backward rotation. For example, in Fig. 2 *b*, an applied torque of 1% was sufficient to stop the cell in the CW mode, whereas torques greater than about 3% were required to make it spin CCW. Similarly, an applied torque of -1% was sufficient to stop the cell in the CCW mode, and a torque of $\sim -3\%$ was required to make it spin CW. In addition, motors in both modes displayed approximately the same linear dependence of speed on torque when spinning backward as when spinning forward. The symmetry between the two modes can be seen by rotating Fig. 2 through 180°, which leaves it essentially unchanged.

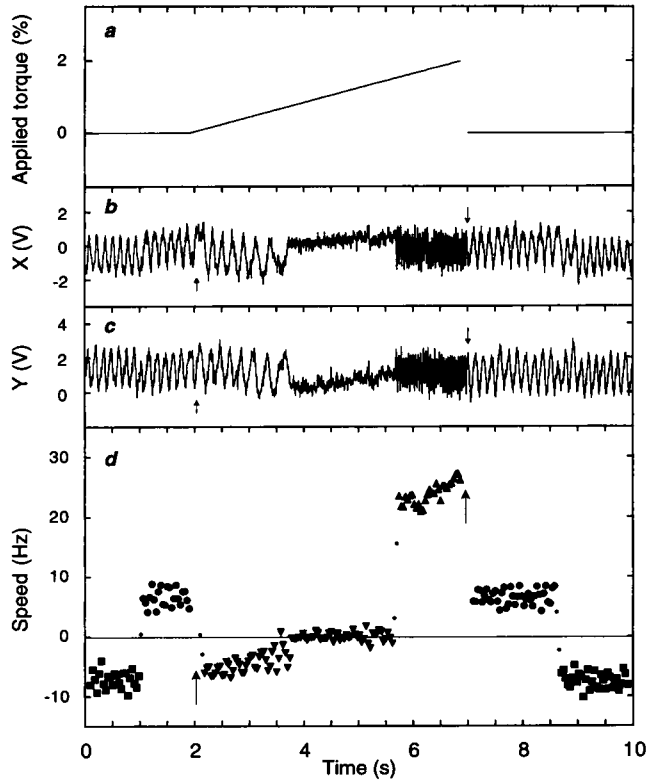

FIGURE 1 Rotation of a single tethered cell of strain KF84 under externally applied torque. (a) Applied torque as a percentage of the maximum possible with our apparatus; (*b* and *c*) output voltages corresponding to the x- and y-positions of the center of mass of the cell image; and (*d*) cell rotation rate, each as functions of time. In the CW mode, the cell rotated near -7 Hz in the absence of external torque (■) and slowed to a stop when an opposing CCW torque was applied (▼). In the CCW mode, the cell rotated near $+7$ Hz and above $+20$ Hz without (●) and with (▲) external torque, respectively. Arrows in (*b–d*) indicate the beginning and end of application of external torque. Points appear between modes as a result of smoothing of calculated speeds when the motor switched.

Catastrophic breaking

Berg and Turner (1993) identified catastrophic breaks from the sudden increase in the speed of a cell resisting an externally applied torque and from the failure of such a cell to spin again when the external torque was switched off. Here we used the same strain of *E. coli* tethered identically and subjected to external torque using the same apparatus, but with a modified experimental procedure to examine more closely the nature of these breaks. Cells of strain KF95, whose motors operate exclusively in the CCW mode, were subjected to steadily increasing CW torques while

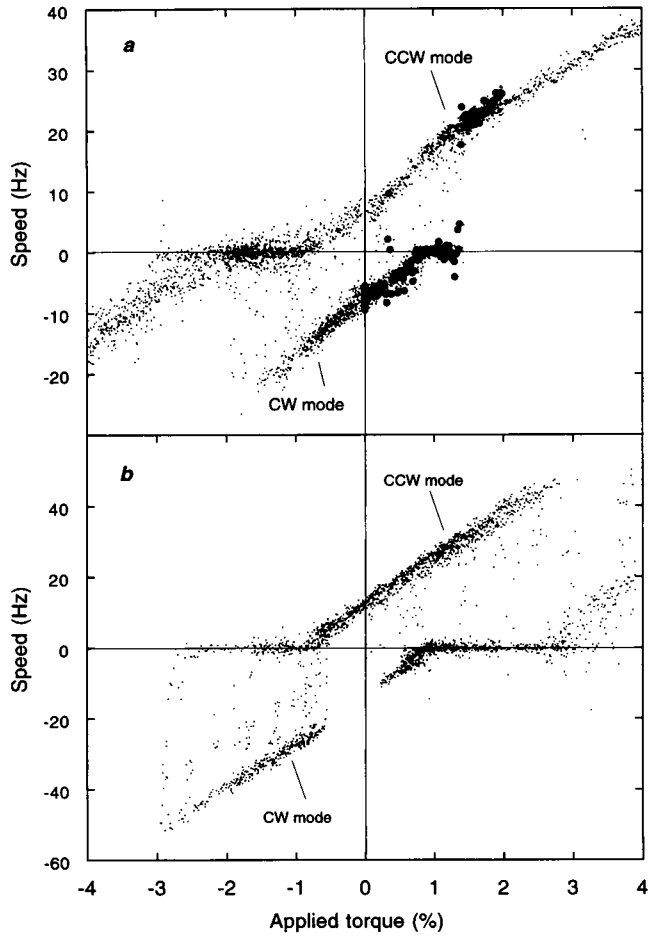

FIGURE 2 Rotation speeds of two cells of strain KF84 as functions of applied torque. Progressively larger torques in alternating directions were applied as an experiment progressed. Each cell exhibited two rotational modes, both of which showed the same dependence of speed on torque. The bold dots in (*a*) are the data shown in Fig. 1 *d*. This cell had a tendency to switch to the CCW mode at higher applied torques, a behavioral response to heating (Maeda et al., 1976) caused by the electric field. This response was reversed in (*b*) by incubation of cells in 1 mM serine, 0.5 mM aspartate (Mizuno and Imae, 1984) to reveal more of the CW mode. Scattered points between the modes are due to smoothing of sudden changes in speed when the motor switches (Fig. 1).

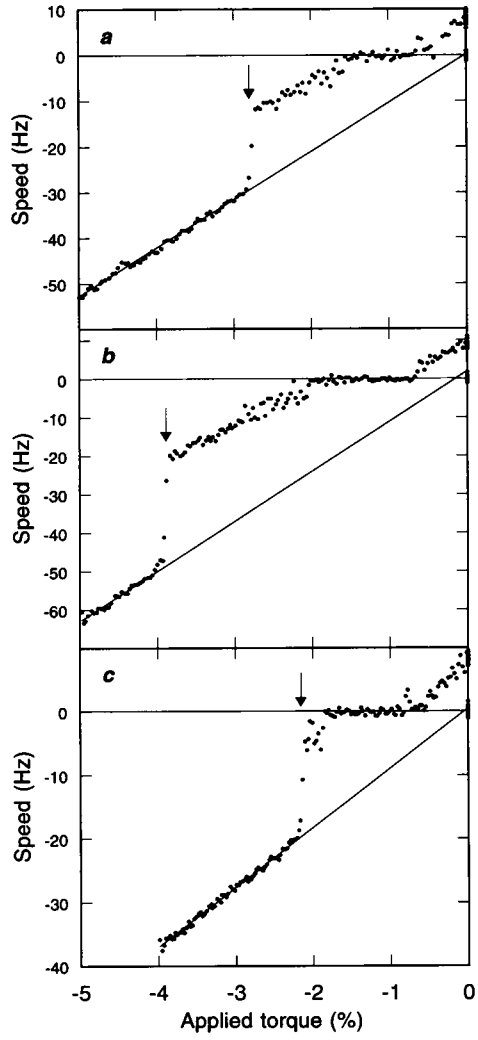

FIGURE 3 Speed as a function of applied torque for three cells of strain KF95 broken catastrophically by externally applied torque. Steadily increasing CW torque was applied while cell speed was monitored, as illustrated in Fig. 1. The lines are least-squares linear fits to points obtained after the cells had broken. These lines extrapolate to the origin, indicating that broken motors do not generate torque. When external torque was removed, cells stopped rotating.

their speed was monitored, in the manner illustrated in Fig. 1. Speed was plotted as a function of torque as before, but now for single rather than multiple runs.

Fig. 3 shows three examples of motors broken catastrophically. In these plots, the fate of the cell unfolds from right to left. Increasing torque slowed a cell to a halt, held it at stall, pushed it backward, and finally broke it (*arrows*). Line fits to speeds obtained after the break extrapolate to the origin, indicating that a cell with a broken motor exerts only passive, frictional resistance to rotation. Also, when the applied torque was switched off, a cell stopped rotating but continued to exhibit rotational Brownian motion. If the change in the resistance in the motor due to the break is negligible compared with the drag on the cell body, as assumed in earlier work (Berg and Turner, 1993), then the fitted line gives the speed at which the cell would spin in the absence of any motor torque. Thus at a given applied torque, the torque generated by the intact motor is proportional to the difference between the speed recorded when the motor was intact and the speed recorded after it was broken (called the "speed offset"). This follows because the Reynolds number is very small, so that the speed of a cell is strictly proportional to the total torque acting on it.

In terms of the torque generated by the motor, the data in Fig. 3 can be interpreted as follows. Initially, the motors all generated a constant torque, T_0. This torque remained roughly constant as a motor was slowed to a stop by the applied torque, and then it increased by a factor of 2 or 3 to a maximum value, T_{max}, while the motor was stalled. Then the motors began to rotate backward, resisting with torque approximately equal to T_{max}. This continued until the motor broke, after which it exerted zero torque. The breaks oc-

curred at different speeds (about −10, −20, and −5 Hz for the cells shown in Fig. 3, *a*, *b*, and *c*, respectively). Cells broken in this way (with a sudden transition to zero torque) were observed for 10 min after breaking, during which time they failed to recover. We conclude that the high torque, T_{max}, which cells exert when pushed backward, is sufficient to break some series element, presumably in the chain that links the site of torque generation to the flagellar filament.

Progressive breaking

Berg and Turner (1993) also described breaks in which the torque generated by motors was reduced in stages as cells were repeatedly pushed backward. Fig. 4 illustrates this behavior. The cell in Fig. 4 *a* was pushed backward, as described in Fig. 1, but repeatedly. Midway through the first run (*open circles*), the motor was partially broken such that the torque it exerted was approximately halved. Notice that this cell recovered somewhat, immediately after the break. The second run (*closed circles*) was made immediately afterward and shows speed as a function of applied torque for this partially broken motor. As before, the motor exerted constant torque while spinning forward and constant but considerably higher torque while spinning backward and was stalled at intermediate torques. The only difference between the intact and partially broken motor was that the latter exerted less torque. Fig. 4 *b* shows cell speed as a function of applied torque for a second cell treated in a similar manner. During the first run (*open circles*), the motor was intact and showed the characteristic torque versus speed relationship described in the previous section. The motor was broken progressively during subsequent runs (not shown) and on the eighth run (*closed circles*) showed a similar torque versus speed relationship, only with reduced motor torque.

Fig. 5 shows the progressive breaking of another cell over a time span of about 10 min. The cell was pushed backward a total of six times. The speeds displayed were recorded as the cell spun under its own power between pushes. Each push broke the motor progressively more, until at about 700 s it stopped rotating entirely. Notice that after the last push the speed of the cell decreased on its own to zero; this behavior was typical of cells broken progressively. Then the cell began to rotate sporadically, and about a minute later it had recovered well enough to rotate steadily at about half its original speed. Fig. 5 *b* is a histogram of the speeds shown in Fig. 5 *a*. Clearly, the cell rotated predominantly at certain discrete speeds. If progressive breaking involves the removal or destruction of individual torque-generating units, we would expect the cell to spin at integral multiples of the speed due to a single unit, as the number of intact units in the motor is progressively reduced. Fig. 5 *b* shows that the data are consistent with this prediction.

Recovery after progressive breaking

Our hypothesis is that progressive breaking disrupts MotA/MotB torque-generating units, leaving the rest of the motor intact. Thus we might expect motors broken progressively to recover in steps similar to those seen in the resurrection of *mot*$^-$ strains by plasmid-encoded *mot*$^+$ genes (Block and Berg, 1984; Blair and Berg, 1988), as torque-generating units are either repaired or replaced, one by one. This is indeed the case, as is shown in Fig. 6 *a*. This cell was partially broken by a single backward push, and it came to a halt at $\sim t = 100$ s. About a minute later, it began to rotate at $\sim$ 1/11 of its original speed, then increased in steps to two, three, and four times the slowest speed. The cell rotated for several minutes at each of the third and fourth speed levels (data not shown). The cell in Fig. 6 *b* recovered

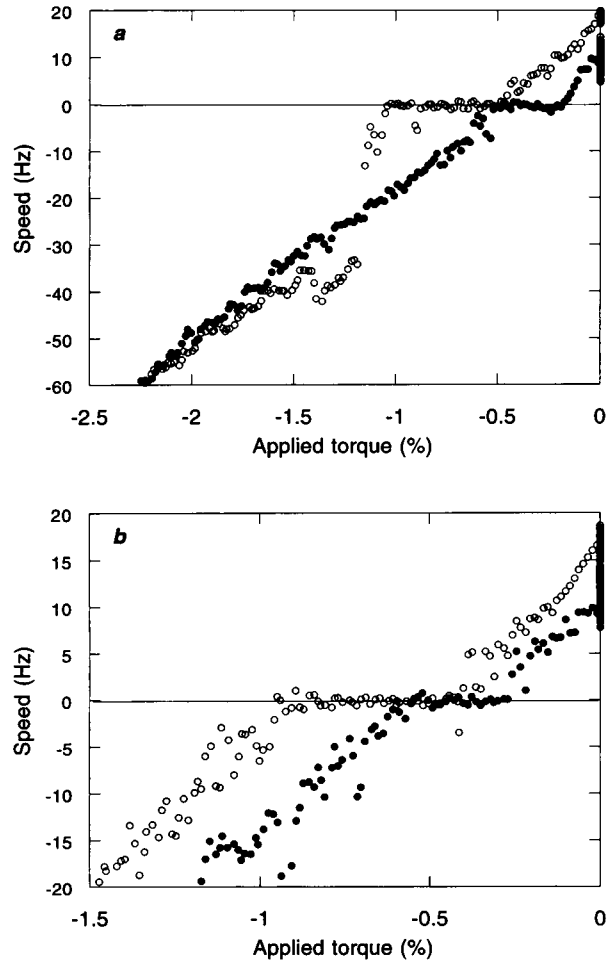

FIGURE 4 Speed as a function of applied torque for two cells of strain KF95 broken progressively by external torque. Open circles (○) are for the first run where torque was applied to a cell, and filled circles (●) are for subsequent runs where torque was applied to the same cell. (*a*) Before any external torque was applied, this cell rotated at just below 20 Hz. An applied torque of −0.5% stopped the cell, and an applied torque of −1% made it rotate backward. At this point the cell broke, speeding up suddenly from 15 to 35 Hz. However, the cell did not break completely. The torque after the break was not zero, and the cell rotated at about 10 Hz when the field was turned off. The second run was taken a few seconds later and shows speed as a function of applied torque for the partially broken motor. (*b*) The motor of this cell was unbroken during the first run, but by the eighth run the motor had been partially broken by several progressive breaks, similar to the one shown in (*a*).

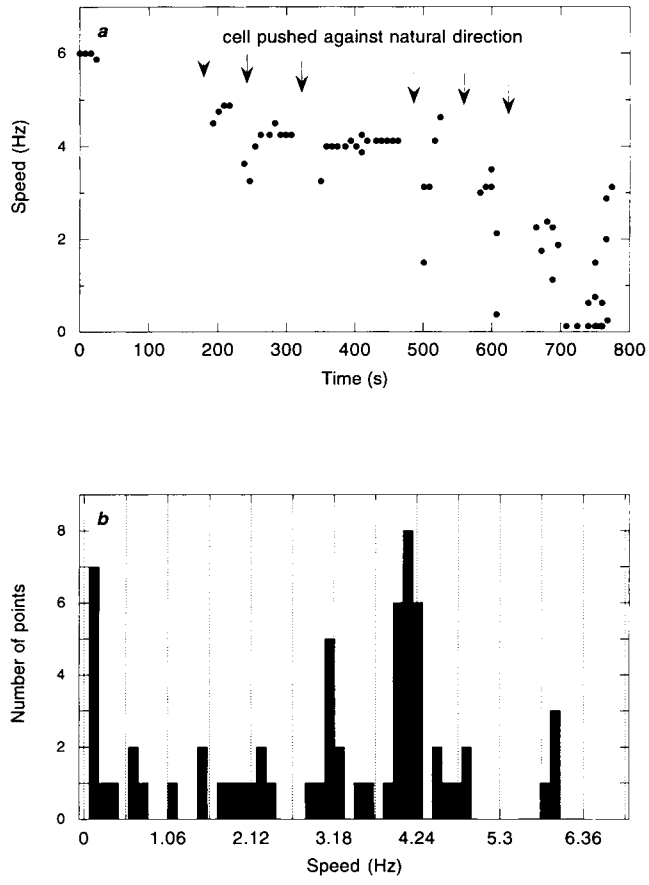

FIGURE 5 (*a*) The speed of a single cell of strain KF95, rotating under its own power, for several minutes during which the cell was progressively broken. Arrows indicate times at which torque was applied to push the cell backward. After each push, the cell rotated a little more slowly than before, but it did not stop completely until after the sixth push. It began to recover within a minute. (*b*) A histogram of the data in (*a*) showing the distribution of speeds at which this cell spun while being broken progressively. Vertical grid lines are drawn at intervals of 0.53 Hz to guide the eye. The cell seemed to rotate predominantly at integral multiples of this speed. The data for this figure were analyzed over successive 8-s intervals via complex power spectra, as described in Materials and Methods.

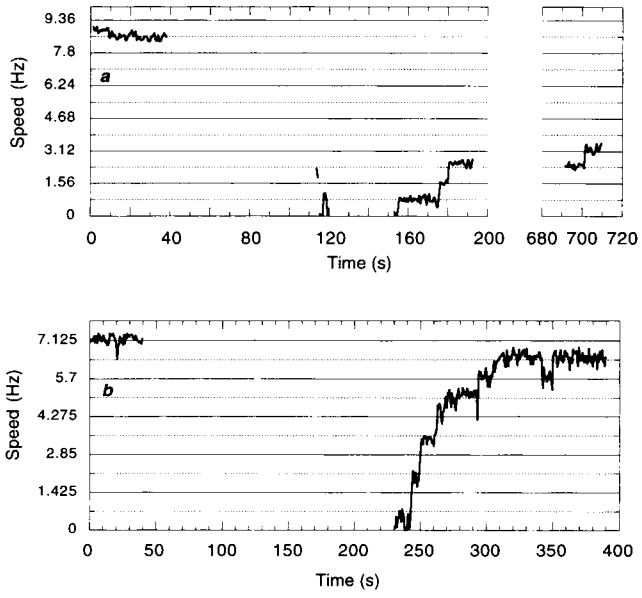

FIGURE 6 Speed versus time for two cells of strain KF95 recovering after progressive breaking. The data starting at time 0 were obtained before external torque was applied. Subsequent data were obtained after the cell had been broken to the point where it had stopped rotating under its own power. The speed of the cell in (*a*) remained approximately constant between t = 190 s and t = 690 s, and also for several minutes after t = 710 s.

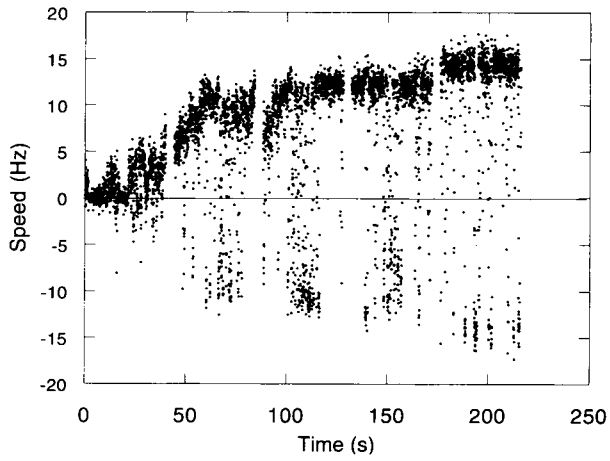

FIGURE 7 Speed versus time for a cell of strain KF84 (wild-type for chemotaxis) recovering after progressive breaking. This cell had a considerable CCW bias, but rotated CW often enough to demonstrate that the time course for recovery of both directional modes was the same.

considerably faster than the cell in Fig. 6 *a*, and in this respect was more typical of recovering cells in other experiments. For this reason, steps in the speed of the recovering cell are not so clearly visible as in Fig. 6 *a*. Nevertheless, the data show abrupt changes in speed by 1/5 ($\sim t$ = 250 s) and 1/10 ($\sim t$ = 350 s) of the original speed of the cell. These data support the hypothesis that motors broken progressively are able to recover by restoring functional torque-generating units, and they raise the question of the number of units present in a fully operational motor. We will return to this point in the Discussion.

Fig. 7 shows speed versus time for a switching cell (strain KF84) recovering after having been broken progressively by negative (CW) applied torque. This cell had a considerable CCW bias, but it is clear that speeds in either direction increased together. This is consistent with results from the *mot* resurrection experiments (Block and Berg, 1984; Blair and Berg, 1988), which showed that each torque-generating unit can rotate a cell in either direction. We saw progressive breaks in switching cells pushed backward in either mode but catastrophic breaks only in the CCW mode, probably because cells tended to switch out of the CW mode at high, applied torques. This was a thermal response to heating by the electric field: unless preadapted to serine and aspartate, wild-type cells spin CCW when exposed to sharply increasing temperatures (Maeda et al., 1976; Mizuno and Imae, 1984). On several occasions, a cell spinning fast in the CCW mode under a CCW applied torque would switch

modes so that it was suddenly trying to spin against the applied field. Such cells would often partially break before switching back, at which point they could be seen to generate reduced torque. Clearly cells were not deterred from switching into a mode where they might be broken. In general, cells were seen to switch both into and out of either mode, whether they were spinning forward, were stalled, or were being forced backward in that mode.

In summary, these data show that progressive breaking involves the removal of independent torque-generating units from the motor. These units may be repaired or replaced over the course of seconds to minutes. In addition, partially broken motors, presumably containing a reduced number of functional torque generators, show the same dependence between torque and speed as do intact motors, at least at low speeds. This indicates that the torque-speed relationship is characteristic of the torque generators themselves and is neither an artifact of the technique nor due to other components of the motor. We were not able to predict when a cell would break or whether it would break catastrophically or progressively.

DISCUSSION

Before the electrorotation experiments presented in this and the previous work, it was believed that torque decreased linearly with speed in the forward direction (Lowe et al., 1987). There were no data on cells resisting backward rotation. The electrorotation experiments show that the motor generates approximately constant torque in the forward direction up to a particular, temperature-dependent speed, above which the torque drops steadily (Berg and Turner, 1993). When rotating backward, the motor also generates constant but considerably higher torque. In both the present and the previous work, the ratio of the maximum torque to the stall torque is highly variable. There remains the possibility that broken and deenergized motors do not have negligible frictional drag, as we have assumed. If this were true, the reference state would underestimate the speed of a cell rotating with no motor torque, so that the speed offset would overestimate the motor torque. Assuming that the additional frictional drag was proportional to velocity, this would mean that motor torque actually decreases linearly with speed, both in the forward direction and when motors are forced backward. Nevertheless, the discontinuity in motor torque between forward and backward rotation would remain.

The ability to predict the correct torque-speed relationship is an important test of any model of the bacterial flagellar motor. It will be interesting to see whether existing models can be adapted to match the new data or whether a new model is needed. The resistance of the motor to backward rotation favors models in which rotation and proton flux are tightly coupled. In a tightly coupled model, if the transit of protons in the reverse direction (out of the cell) is an extremely slow process whose rate is independent of torque, then the motor will resist backward rotation. However, the constant high torque limit observed when the motor is driven backward fits less well with a tightly coupled model. It is not impossible that the energy available at high torque is enough to pump protons out of the cell and that there is a threshold torque for this, but it seems more likely that tight coupling breaks down and the motor slips without pumping protons. In this event, the motor might be described by a model that is tightly coupled but allows for slippage (Kleutsche and Läuger, 1990) or by a model that is loosely coupled but exhibits tight coupling over certain parameter ranges (Berry, 1993). We do not understand the wide variation in the observed values of maximum torque, but this variation might indicate that backward rotation follows some kind of mechanical failure that differs from one motor to the next.

Ideally, a new model should also allow for switching between symmetrical directional modes. It seems unlikely that there are separable CW and CCW torque generators, as the torques observed during resurrection and breaking and recovery have always been the same in either mode. Two types of mechanisms have been proposed to explain how the bacterial flagellar motor couples influx of ions to torque yet can rotate in either direction. Neither type necessarily gives symmetrical torque generation. In one, conformational changes reverse the basic geometrical asymmetry that underlies torque generation. For example, in the model of Läuger, where protons are constrained to move at the intersection of half channels on the rotor and stator, switches occur when the relative tilt of these half channels reverses (Läuger, 1977, 1988; Kleutsche and Läuger, 1990). In the other type of mechanism, switching is achieved by changing the effect of protonating functional groups in the motor, so that in one mode protonation makes neutral basic groups positively charged, whereas in the other, protonation makes negatively charged acidic groups neutral. For example, in the model of Berry (1993), in which torque is generated by attraction between charges flowing through channels on the stator and tilted lines of complementary charges on the rotor, positive charges flow into the cell in one mode, and negative charges (holes) flow out of the cell in the other. Alternatively, in the model of Berg and Khan (1983), the direction of torque can be reversed if the constraints on the motion of stator elements depend on whether specific sites on the rotor are charged, rather than on whether they are protonated (Meister et al., 1989). Our results show that motor torque is symmetrical over a wide dynamic range, so that whatever the mechanism of switching might be, the physical process that generates torque is quantitatively the same in either directional mode.

Our results also raise the question of the nature of the interaction between the rotor and stator in the bacterial flagellar motor. Progressive breaking and recovery of the motor in discrete steps is further evidence of the independence of the torque-generating units, but it is not clear whether progressive breaks destroy units, leaving them in place, or whether it is the association between the torque generators and the rotor that is disrupted. The observation that partially broken motors run

down to zero torque on their own, after progressive breaking, supports the latter hypothesis; pushing the motor backward might weaken some part of the link between the site of attachment to the cell wall and the site of interaction with the rotor, so that units generate torque intermittently before becoming detached completely. As for catastrophic breaking, we might speculate that it is the connection between the C-ring and the MS-ring that gives way. This would explain why cells with broken motors remain well tethered, as the MS-ring would prevent the flagellar filament from slipping out of the cell envelope. The difficulty of isolating motors without losing the C-ring and the extremely faint appearance of the connection between the C-ring and the rest of the flagellum in electron micrographs (Francis et al., 1994) also invite speculation that this connection is the weak link in the chain between the torque generators and the filament. It is still possible that other components, for instance the rod, can also break catastrophically. If the rod were to break, we would expect the cells to come off the glass, leaving the filament, hook, and broken rod behind (Okino et al., 1989). Loss of tethered cells was observed in both sets of electrorotation experiments. Of course, an alternative explanation for this loss is that the covalent linkage of filaments to the surface is not always strong enough to hold cells at high speeds.

Another question raised by experiments on progressive breaking is the number of torque-generating units in a normal motor. Early resurrection experiments (Block and Berg, 1984) estimated 16, based on the ratio of speeds of single-unit and wild-type motors and also on the number of particles seen in freeze-fracture electron micrographs (Coulton and Murray, 1978). However, the later resurrection experiments (Blair and Berg, 1988) revealed eight steps at most, and the speeds of eight-unit motors were comparable to those of wild-type motors. Our results suggest the possibility that there might be more than eight units per motor, based on a comparison between speed increments in recovering motors and the speeds of the same motors before breaking. For example, the speed increments for the cell in Fig. 6 are 1/11 of the original speed of the cell. In view of the double-headed nature of the eukaryotic motor protein kinesin, it is tempting to suggest that motor molecules in the flagellar motor normally travel in pairs. This would explain the disparity between the number of steps seen in resurrecting motors and the number of studs seen in electron micrographs. Our results would follow if it were possible to break one of a pair without breaking the other. This would explain the two step sizes visible in our Fig. 6 *b*. Large steps show the recovery of intact pairs, small steps show the recovery of pairs with one member broken. However, without knowledge of the structure and stoichiometry of the torque-generating units, this discussion remains highly speculative.

We thank Karen Fahrner for the strains KF84 and KF95 and for comments on the manuscript.

Richard M. Berry is supported by a Wellcome Trust International Prize Travelling Research Fellowship. This work was supported by the Rowland Institute for Science.

REFERENCES

Berg, H. C. 1974. Dynamic properties of bacterial flagellar motors. *Nature (Lond.)*. 249:77–79.

Berg, H. C., and S. Khan. 1983. A model for the flagellar rotary motor. *In* Mobility and Recognition in Cell Biology. H. Sund and C. Veeger, editors. deGruyter, Berlin. 485–497.

Berg, H. C., and L. Turner. 1993. Torque generated by the flagellar motor of *Escherichia coli*. *Biophys. J.* 65:2201–2216.

Berry, R. M. 1993. Torque and switching in the bacterial flagellar motor: an electrostatic model. *Biophys. J.* 64:961–973.

Blair, D. F. 1990. The bacterial flagellar motor. *Semin. Cell Biol.* 1:75–85.

Blair, D. F., and H. C. Berg. 1988. Restoration of torque in defective flagellar motors. *Science (Washington DC)*. 242:1678–1681.

Block, S. M., and H. C. Berg. 1984. Successive incorporation of force-generating units in the bacterial rotary motor. *Nature (Lond.)*. 309: 470–472.

Conley, M. P., and H. C. Berg. 1984. Chemical modification of *Streptococcus* flagellar motors. *J. Bacteriol.* 158:832–843.

Coulton, J. W., and R. G. E. Murray. 1978. Cell envelope associations of *Aquaspirillum serpens* flagella. *J. Bacteriol.* 136:1037–1049.

Francis, N. R., G. E. Sosinsky, C. Thomas, and D. J. DeRosier. 1994. Isolation, characterization and structure of bacterial flagellar motors containing the switch complex. *J. Mol. Biol.* 235:1261–1270.

Fröberg C. E. 1969. Introduction to Numerical Analysis, 2nd ed. Addison-Wesley, Reading, Massachusetts. p. 190.

Fung, D. C., and H. C. Berg. 1995. *Nature (Lond.)*. In press.

Jones, C. J., and S.-I. Aizawa. 1991. The bacterial flagellum and flagellar motor: structure, assembly and function. *Adv. Microb. Physiol.* 32: 109–172.

Khan, S., M. Dapice, and I. Humayun. 1990. Energy transduction in the bacterial flagellar motor: effects of load and pH. *Biophys. J.* 57: 779–796.

Khan, S., M. Meister, and H. C. Berg. 1985. Constraints on flagellar rotation. *J. Mol. Biol.* 184:645–656.

Khan, S., T. S. Reese, and M. Dapice. 1988. Effects of *Mot* gene expression on the structure of the flagellar motor. *J. Mol. Biol.* 202:575–584.

Kleutsche, B., and P. Läuger. 1990. Coupling of proton flux and rotation in the bacterial flagellar motor: stochastic simulation of a microscopic model. *Eur. Biophys. J.* 16:175–191.

Läuger, P. 1977. Ion transport and rotation of bacterial flagella. *Nature (Lond.)*. 268:360–362.

Läuger, P. 1988. Torque and rotation rate of the bacterial flagellar motor. *Biophys. J.* 53:53–65.

Lowe, G., M. Meister, and H. C. Berg. 1987. Rapid rotation of flagellar bundles in swimming bacteria. *Nature (Lond.)*. 325:637–640.

Macnab, R. M. 1992. Genetics and biogenesis of bacterial flagella. *Annu. Rev. Genet.* 26:131–158.

Maeda, K., Y. Imae, J.-I. Shioi, and F. Oosawa. 1976. Effect of temperature on motility and chemotaxis of *Escherichia coli*. *J. Bacteriol.* 127: 1039–1046.

Manson, M. D., P. M. Tedesco, and H. C. Berg. 1980. Energetics of flagellar rotation in bacteria. *J. Mol. Biol.* 138:541–561.

Meister, M., S. R. Caplan, and H. C. Berg. 1989. Dynamics of a tightly coupled mechanism for flagellar rotation. *Biophys. J.* 55:905–914.

Meister, M., G. Lowe, and H. C. Berg. 1987. The proton flux through the bacterial flagellar motor. *Cell.* 49:643–650.

Mizuno, T., and Y. Imae. 1984. Conditional inversion of the thermoresponse in *Escherichia coli*. *J. Bacteriol.* 159:360–367.

Okino, H., M. Isomura, S. Yamaguchi, Y. Magariyama, S. Kudo, and S.-I. Aizawa. 1989. Release of flagellar filament-hook-rod complex by a *Salmonella typhimurium* mutant defective in the M ring of the basal body. *J. Bacteriol.* 171:2075–2082.

Schuster, S. C., and S. Khan. 1994. The bacterial flagellar motor. *Annu. Rev. Biophys. Biomol. Struct.* 23:509–539.

Silverman, M., and M. Simon. 1974. Flagellar rotation and the mechanism of bacterial motility. *Nature (Lond.)*. 249:73–74.

Washizu, M., Y. Kurahashi, H. Iochi, O. Kurosawa, S.-I. Aizawa, S. Kudo, Y. Magariyama, and H. Hotani. 1993. Dielectrophoretic measurement of bacterial motor characteristics. *IEEE Trans. Ind. Appl.* 29:286–294.